ISBN: 978-3-95450-224-0 ISSN: 2673-7035 doi:10.18429/JACoW-FLS2023-TU4P07

DESIGN OF THE BEAM DISTRIBUTION SYSTEM OF SHINE*

S. Chen†, X. X Fu, H. X. Deng, B. Liu, Shanghai Advanced Research Institute, Shanghai, China
B. Y. Yan, University of Chinese Academy of Sciences, Beijing, China

Abstract

For feeding the three parallel undulator lines by the CW beam of a single SRF linac simultaneously, a beam switchyard between the linac and undulator lines is designed with the consideration of bunch-by-bunch beam separation and beam quality per. In this work, the schematic design of the beam switchyard for bunch-by-bunch beam separation of CW beam is described, and the current lattice design of the linac-to-undulator deflection branches and the start-to-end tracking simulation results are presented.

INTRODUCTION

As a high repetition rate XFEL and extreme light facility, the SHINE project is now under construction near the SSRF and ShanghaiTech campus [1,2]. High quality electron beam is generated by a VHF gun in CW mode with a repetition rate up to about 1 MHz [3]. A superconducting RF linac with two bunch compressors then accelerates the electron beam to about 8 GeV. The electron beam is used to feed the FEL undulator complex with three parallel undulator lines, referred to as FEL-I (3-15 keV), FEL-II (0.4-3 keV) and FEL-III (10-25 keV) respectively. In addition, spaces are reserved for future upgrade of more undulator lines.

For the simultaneous operation of multiple undulator lines with different parameters and operation modes in SHINE, a beam switchyard is located in between the SRF linac and the undulator lines complex. In the beam switchyard, he 1 MHz CW electron beam should be separated bunch-by-bunch in an arbitrarily programmable pattern and then delivered to each undulator line through the corresponding linac-to-undulator (LTU) branch respectively. In this work, we present the physics design of the beam switchyard for SHINE.

MAIN LAYOUT

A schematic view of the SHINE is seen in Fig. 1. Most of the beam equipment will be installed in the tunnels and shafts about 30 m underground. Electron beam starts from the injector in #1 shaft and is accelerated by the SRF linac in a 1.4 km long tunnel. The three undulator lines are installed in two of the undulator tunnels: FEL-I and FEL-II in the middle undulator tunnel and FEL-III in the west undulator tunnel. All the three undulator lines are parallel to the linac line, in the same vertical plain but not collinear. The horizontal distance between the three undulator line and the linac is about +1.85 m for FEL-II, -1.45 m for FEL-I and -8.95 m for FEL-III, where '+'('-') denotes left(right) to the linac beam direction. The linac tunnel and the undulator tunnels are connected by the #2 shaft. Some key beam parameters of SHINE are listed in Table 1.

Table 1: SHINE Main Beam Parameters

Parameter	Value	Unit
Beam Energy (E_0)	8.0	GeV
Slice Energy Spread (σ_E/E_0)	~0.01	%
RMS Norm. Emittance (ε_n)	≤0.45	μm · rad
Bunch Frequency (f_{rep})	1000	kHz
Bunch Charge (Q)	10~300	pC
Bunch Length (l_b)	~100	fs
Peak Current (I_{pk})	≥1500	A

The beam switchyard section starts from the end part of the linac tunnel, passes through the #2 shaft and ends at the entrance of the undulator lines. Electron bunches from the linac should be separated and delivered either to the three undulator lines or to a 800-kW beam dump in the middle of #2 shaft. Starts from the end of the SRF linac, a linac-to-dump (LTD) line brings the undeflected bunches to the main dump. Three LTU deflection branches extract bunches from the LTD line in the sequence of LTU-2, LTU-3, and LTU-1. This arrangement avoids the conflict of the three LTU branches and reserves spaces for future extension of more LTU branches for more undulator lines.

KICKER-SEPTUM MODULE

An electron bunch that is wanted by an undulator line should be firstly extracted from the 1 MHz CW electron bunch train without affecting the bunches to other directions. Typically it is realized by pulsed kicker magnets. For maximizing the available beam modes that can be provided to the user experiments and their flexibility of switching, the kicker magnets should be able to perform a stable bunch-by-bunch kick to the electron beam and, what's more, should be programmable for arbitrary distribution pattern. Considering the beam parameter and the limited geometry, a single kicker magnet could not meet the requirements independently. Therefore, the actual scheme is based on a set of small angle vertical kicker magnets combined with a DC Lamberson septum magnet, which can be a compact scheme with high enough frequency and stability.

The configuration of the kicker-septum module is seen in Fig. 2. The fast kicker set and the DC Lamberson septum magnet are inserted in a FODO cell with about 24 m period. The fast kicker set consists of 8(+2) special designed lumped-inductance kicker magnets with a total deflection angle of about 0.8 mrad [4]. The pole of the kicker magnet is out of vacuum so that ceramic vacuum chamber should be used. To reduce the wakefields, the ceramic vacuum chamber should

* Work supported by the Natural Science Foundation of Shanghai (22ZR1470200).
† chens@sari.ac.cn

ISBN: 978-3-95450-224-0 ISSN: 2673-7035 doi:10.18429/JACoW-FLS2023-TU4P07

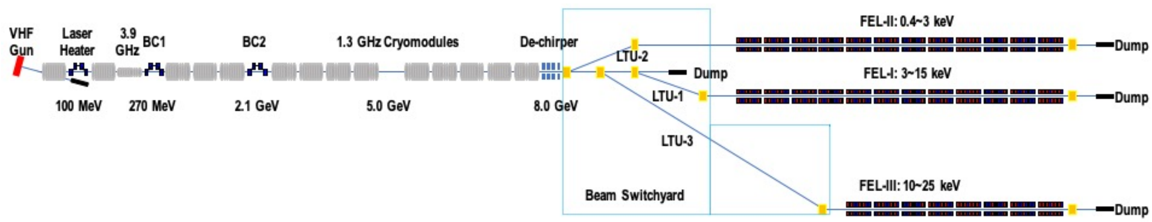

Figure 1: SHINE Schematic Layout

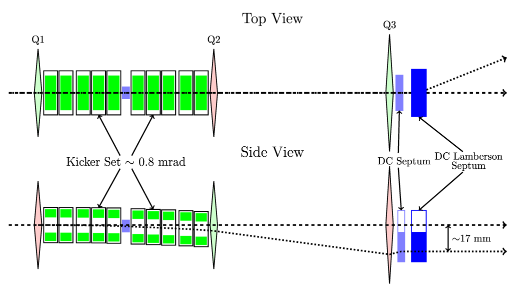

Figure 2: Schematic view of a kicker-septum module.

be coated with a conductive material and the alignment along the kicker set is slightly adjusted to prevent the beam to be too close to the chamber side. In order to ensure the relative beam trajectory stability $< 0.1\sigma_{x,y}$, it is required that the repetitive stability of the magnetic field of the kicker magnet be below 100 ppm.

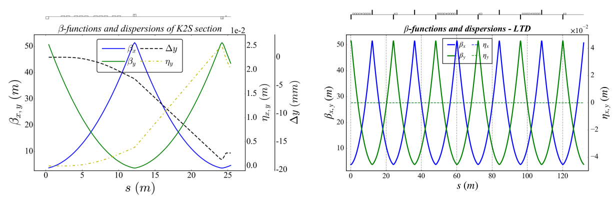

Figure 3: Lattice functions of the kicker-septum modules.

The quadrupoles of the FODO cells are aligned to be centering with the non-kicked straight bunch so that the kicked bunch experiences an extra deflection while passing them off-axis. The vertical angle of the bunch is eliminated by a small DC septum and the bunch then enters the DC Lamberson septum with ~17 mm vertical offset to the un-kicked bunch for further horizontal deflection. Because of the limited longitudinal space available for beam switchyard, the kicker-septum section is designed to be modularized so that all the three LTU branches share the same kicker-septum configuration, as is seen in the right figure of Fig. 3. For radiation safety reason, beam position monitors and beam collimators should be installed in front and behind the kicker set in order to protect the kickers and the septa. What's more, in case of emergency, all the kickers are switched off immediately to lead all the electron beam to the main dump until the beam is aborted upstream.

LINAC-TO-UNDULATOR BRANCHES

After being separated by the kicker-septum section, the electron bunches are then delivered by the three LTU branches to the corresponding undulator lines respectively. Based on the relative geometric relation between the linac and the three undulator lines, in all the three LTU branches, electron bunches should firstly be deflected to the direction of the undulator lines by a horizontal dog-leg. In this process, special concern should be given to various collective effects of high-intensity electron beam being deflected, such as the emittance growth due to dispersion effect and coherent synchrotron radiation (CSR) effect, the micro-bunching instability that may spoil the longitudinal phase space. For preserving the beam quality, several integrated optics measures are adopted for suppressing those collective effects in the lattice design of the LTU branches. The lattice functions of the three LTU branches are shown in Fig. 4.

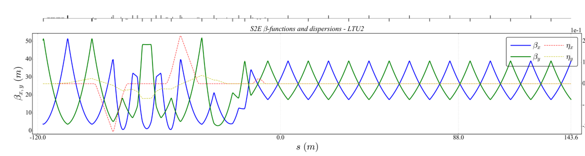

(a) LTU-2

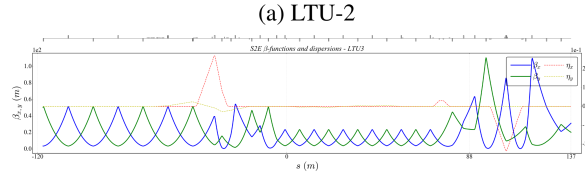

(b) LTU-3

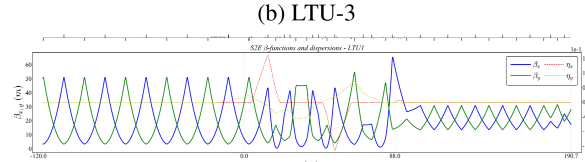

(c) LTU-1

Figure 4: Lattics functions of the three LTU branches.

A direct approach of reducing the CSR effect is by reducing the deflection angle and the beam size at the bending magnet. The deflection part of each LTU branch is designed to be a dual-DBA dog-leg, i.e., replace the two reverse angle bend of the dog-leg by two reverse angle double-bend-achromatic cells for halving the deflection angle of a single bend (1.5° for LTU-2, 1.8° for LTU-3 and 1.0° for LTU-1). The optics of the dog-leg is designed to be mirror symmetrical with a

ISBN: 978-3-95450-224-0 ISSN: 2673-7035 doi:10.18429/JACoW-FLS2023-TU4P07

small β_x (~5 m at the middle of the DC Lamberson septa, which is determined by the FODO of kicker-septum module) at each bend. In addition, a more effective approach of further suppressing the CSR emittance growth is by matching the betatron phase advance between two adjacent dipoles to be an odd multiple of π in the deflection direction, i.e., the optics balance method [5]. To implement this method more effectively, the lattice function of the whole dog-leg is designed to be symmetrical for almost the same CSR kick in all the dipole magnets.

While deflecting the beam in the horizontal direction, the vertical offset and dispersion introduced by the kickers remain. These will be corrected by a small-angle vertical dog-leg after the horizontal dog-leg. At this point, the beam is dispersion-free both horizontally and vertically and heads towards the direction of the undulator line. A series of periodic FODO cells with 16/20 m period and $\pi/4$ phase advance then brings the beam to the entrance of undulator line. In this FODO section, the beam diagnostics instruments, such as beam profile monitors and wire scanners are inserted for emittance and twiss parameter measurement. Besides, in order to protect the radiation sensitive equipment such as the permanent magnet undulators, a final post-linac collimation should be done in advance of the beam entering the undulator lines. There will be an energy collimator inserted in the middle of the first DBA cell of the horizontal dog-leg for eliminating the large off-momentum electrons and several halo collimators inserted in the $\pi/4$-phase-advance FODO cells for removing the halo electrons that may lost in the undulator sections. All the collimators are designed to have adjustable gap to meet with different beam conditions.

START-2-END TRACKING

A collaborated start-2-end tracking simulation is done based on the baseline beam parameter of SHINE. The electron bunch is generated by the VHG gun with optimized parameters and accelerated by the injector and the SRF linac to the entrance of the beam switchyard with the longitudinal phase space distribution shown in Fig. 5. The simulation is done by the particle tracking code ELEGANT [6].

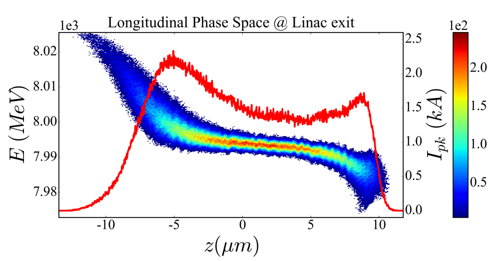

Figure 5: Longitudinal phase space at the exit of linac.

The evolution of the normalized emittance of the three LTU branches is shown in Fig. 6. With the properly designed optics for dispersion free and CSR suppression, both the horizontal and vertical normalized emittance are well preserved after the beam passing through the beam switchyard with the maximum emittance growth less than 5%.

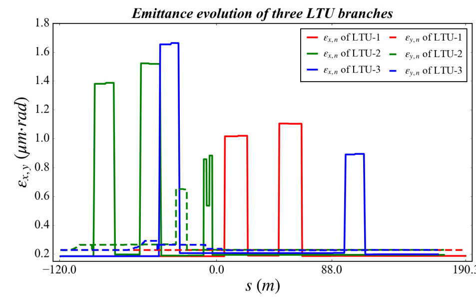

Figure 6: Evolution of emittance along the three LTU branches.

Another important beam dynamic issue of beam switchyard is the micro-bunching instability. For suppressing the micro-bunching growth in the beam switchyard of SHINE, a chicane with adjustable R_{56} is inserted in the proper position on each LTU branch. For LTU-1 and LTU-2, it is inserted in the drift space between the two quadrupoles of the FODO section after the deflection part. For LTU-3, it is inserted in the long matching section between the two DBA cells. The evolution of R56 of the three LTU branches and a comparison of the $t - x$ phase space between non-isochronous case and isochronous case of the three LTU branches are shown in Fig. 7. For the non-isochronous case, the maximum R_{56} of LTU-1, LTU-2, LTU-3 is about 100, 400, and 650 μm, respectively. Obvious micro-bunching gain can be observed in the phase space for this case, especially for the LTU-3 branch. For the isochronous case, the R_{56} is almost eliminated by the properly set chicane, micro-bunching gain in the phase space is barely observable.

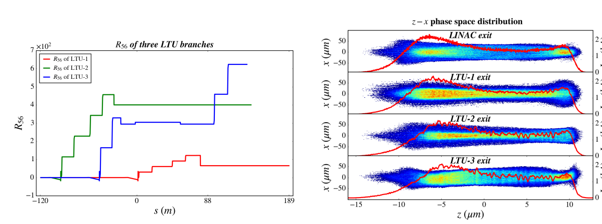

Non-isochronous cases

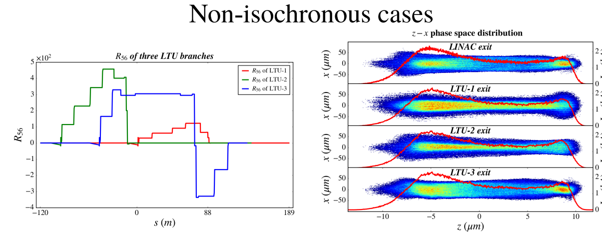

Isochronous cases

Figure 7: Comparison of the current profile at the exit of each LTU branch.

ISBN: 978-3-95450-224-0 ISSN: 2673-7035 doi:10.18429/JACoW-FLS2023-TU4P07

REFERENCES

[1] Z. T. Zhao, D. Wang, Z. H. Yang *et al.*, "SCLF: An 8-GeV CW SCRF linac-based x-Ray FEL facility in Shanghai, in Proc. FEL'17, Santa Fe, NM, USA, MOP055. doi:10.18429/JACoW-FEL2017-MOP055

[2] C. Feng and H.-X. Deng, "Review of fully coherent free-electron lasers", *Nucl. Sci. Tech.*, vol. 29, p. 160, 2018. doi:10.1007/s41365-018-0490-1

[3] H. Chen, L.-M. Zheng, and B. Gao, *et al.*, "Beam dynamics optimization of very-high-frequency gun photoinjector", *Nucl. Sci. Tech.*, vol. 33, p. 116, 2022. doi:10.1007/s41365-022-01105-y

[4] Y. Liu, R. Wang, J. Tong, *et al.*, "Development of a high-repetition-rate lumped inductance kicker magnet prototype for beam switchyard of SHINE, *Nucl. Sci. Tech.*, to be published.

[5] S. Di Mitri, M. Cornacchia, and S. Spampinati, "Cancellation of coherent synchrotron radiation kicks with optics balance", *Phys. Rev. Lett.*, vol. 110, p. 014801, 2013. doi:10.1103/PhysRevLett.110.014801

[6] M. Borland, *Elegant: A flexible SDDS-compliant code for accelerator simulation*, Advanced Photon Source, Argonne National Lab, IL, USA, Rep. LS-287, Sep. 2000.